Published in final edited form as:
Nucl Med Biol. 2008 July ; 35(5): 549–559. doi:10.1016/j.nucmedbio.2007.08.003.

5-*tert*-Butyl-2-(4′-[^{18}F]fluoropropynylphenyl)-1,3-dithiane Oxides: Potential New GABA$_A$ Receptor Radioligands

Xuehe Li, **Yong-Woon Jung**, **Scott E. Snyder**, **Joseph Blair**, **Philip S. Sherman**, **Timothy Desmond**, **Kirk A. Frey**, and **Michael R. Kilbourn**
Department of Radiology, University of Michigan Medical School, Ann Arbor, MI 48109, USA

Abstract

As potential new ligands targeting the GABA receptor ionophore binding site, *trans*-5-*tert*-butyl-2-(4′-fluoropropynylphenyl)-2-methyl-1,1-dioxo-1,3-dithiane **1** and *cis*- and *trans*-5-*tert*-butyl-2-(4′-fluoropropynylphenyl)-2-methyl-1,1,3,3-tetroxo-1,3-dithiane **2** were selected for radiolabeling and initial evaluation as *in vivo* imaging agents for positron emission tomography (PET). Both compounds exhibited an identical high in vitro binding affinity (K_i = 6.5 nM). Appropriate tosylate-substituted ethynyl precursors were prepared by multi-step syntheses involving stepwise sulfur oxidations and chromatographic isolation of the desired *trans*-isomers. Radiolabeling was accomplished in one step using nucleophilic [^{18}F]fluorination. The *in vivo* biodistribution studies with *trans*-[^{18}F]**1** and *trans*-[^{18}F]**2** showed significant initial uptake into mouse brain and a gradual washout, with heterogeneous regional brain distributions and higher retention in cerebral cortex and cerebellum and lower in striatum and pons-medulla. These regional distributions of the new radioligands correlated with in vitro and ex vivo measures of standard radioligands binding to the ionophore- and benzodiazepine-binding sites of the GABA$_A$ receptor in the rodent brain. Comparison of these results with previously prepared radiotracers for other neurochemical targets, including successes and failures as in vivo radioligands, suggests that higher affinity compounds with increased retention in target brain tissues will likely be needed before a successful radiopharmaceutical for human PET imaging is identified.

Keywords

GABA; picrotoxin; tomography; emission-computed; fluorine-18

1. Introduction

γ-Aminobutyric acid (GABA) is the major neurotransmitter in the mammalian central nervous system. The GABA$_A$ receptor is a pentameric protein complex containing binding sites for multiple classes of ligands such as GABA, benzodiazepines, ethanol, barbiturates, neurosteroids, zinc, and non-competitive antagonists such as picrotoxin GABA opens the ion channels and results in an influx of chloride ions, thus hyperpolarizing the membrane and reducing neuronal firing. Deficiencies in GABA-modulated neurotransmission have been implicated in a wide variety of neurological dysfunctions such as epilepsy and other seizure disorders [1–4].

Correspondence to: Michael R. Kilbourn.

In attempts to elucidate the $GABA_A$ receptor function *in vivo* in normal brain and in disease, non-invasive imaging technologies including positron emission tomography (PET) and single photon computed tomography (SPECT) have attracted much interest. Most efforts have been made to develop and validate radiotracers for imaging the benzodiazepine site of the $GABA_A$ receptor [5]. These have resulted in two radiopharmaceuticals, [^{11}C]flumazenil (for PET) and [^{123}I]iomazenil (for SPECT), which have seen extensive human applications. Despite the extensive research on the pharmacology of $GABA_A$ receptors, no suitable radiotracers for any of the numerous additional binding sites are currently available. One such of particular interest is the ionophore (also termed the non-competitive antagonist) binding site, originally identified by the binding of the natural product picrotoxin but which binds a wide variety of compounds with different structures, many of which have been useful as insecticides [6]. Such inhibitors apparently bind to a site associated with the β subunit, with the location of important amino acid residues consistent with a location of the binding site perhaps within the channel of the receptor, and a function of these antagonists to effectively block chloride ion transit through the pore. The ionophore-binding site is associated with $GABA_A$ receptors throughout the brain, and significant occupation of the site produces severe convulsions. A radiotracer designed for the GABA-ionophore binding site might thus provide different and complimentary information to that obtained by the benzodiazepine-based radioligands.

Early attempts to prepare picrotoxin-like radioligands began with labeling the “cage convulsant” compound *tert*-butylbicycloorthobenzoate with fluorine-18 and iodine-125. Although radiochemical syntheses were successful [7–8], these radioligands showed no potential as *in vivo* imaging agents due to rapid hydrolysis in the blood, low brain uptake, and uniform distributions. Subsequent efforts targeted substituted 5-*tert*-butyl-2-phenyl-1,3-dithiane derivatives and their oxides, which have demonstrated much more resistance to hydrolysis and exhibit high biological activity as insecticidal agents acting upon the GABA-ionophore binding site [9–10]. Radiolabeling of this class of molecules was demonstrated using carbon-11, fluorine-18 and iodine-125 [11–12]. In vivo studies with these previous compounds showed adequate blood-brain-barrier penetration and kinetics of uptake and efflux of radioactivity from the brain compatible with short-lived radionuclides, but modest if any regional heterogeneity in radiotracer distribution. Although encouraging, it was felt that the affinities for these initial compounds for the GABA-ionophore binding site were too low (IC_{50} values for in vitro binding uniformly >40 nM) and new, higher affinity molecules would be needed.

The published structure-activity relationship data for the 5-*tert*-butyl-2-phenyl-1,3-dithianes include a variety of aryl ring substituents, sulfur oxidation states, and stereochemistry (both at C-2 carbon and sulfur atoms), with biological data comprised of a mixture of in vitro derived binding affinities (often using different competing radioligands) and in vivo determined toxicities to insects [9,10,13–15]. To help identify potential radioligand candidates, we prepared a short series of representative compounds (Table 1) amenable to labeling with PET radionuclides and evaluated them for in vitro binding affinities using a consistent binding assay with the radioligand [^{3}H]EBOB (4′-ethynyl-4-*n*-[2,3-$^3H_2$]propylbicycloorthobenzoate). Building on our prior experiences, as well as the published structure-activity data [9,10,13–15], interest was then focused on the *trans*-isomers with the 2-methyl substituents and oxidized sulfurs atoms. From this series we identified the 4′-(3-fluoropropynyl)-substituted compounds **1** and **2** as potential candidates for fluorine-18 labeling. To date, these two compounds have shown the highest in vitro binding affinity of any tested in our assays. Labeling with fluorine-18 would be possible using [^{18}F]fluoride ion displacement of a suitably positioned leaving group. Of critical importance was the methyl group at the 2-position of the dithiane ring, which prevents abstraction of the benzylic proton under the basic conditions usually applied for use of nucleophilic [^{18}F]fluoride ion displacements. We report here the synthesis of compounds **1** and **2** in fluorine-18 labeled form and the initial evaluation of their brain uptake in rodents.

2. Materials and Methods

2.1. Animals and chemicals

Mice (CD-1, 20–25 g) were obtained from Charles Rivers. All chemicals were purchased from Aldrich, Inc. and used without further purification unless otherwise noted. *m*-Chloroperoxybenzoic acid was purified by repeated extractions of a CH_2Cl_2 solution with aqueous $NaHCO_3$ to remove m-chlorobenzoic acid before use. Melting points were determined using a hot-stage apparatus and are uncorrected. ^{1}H NMR was performed at 300 MHz. Mass spectra were obtained with EI or ESI techniques. Column chromatography was performed using Davisil® 170–400 mesh silica gel.

No-carrier added [^{18}F]KF was prepared by combining [^{18}F]fluoride, which was produced by proton irradiation of a 2 mL 20% [^{18}O]water target at 20 μA for 10 min, with 200 □L of a5 mg/mL aqueous K_2CO_3 solution and solubolized for reaction by addition of 4,7,13,16,21,24-hexaoxa-1,10-diazabicyclo[8.8.8]-hexacosane (Kryptofix 222). Water was removed by evaporation followed by azeotropic distillation with acetonitrile, and the residue was dissolved in anhydrous DMF for reaction. Radiochemical yields were decay-corrected to the start of synthesis.

2.2. cis-/trans-5-*tert*-Butyl-2-(4′-iodophenyl)-2-methyl-1,1-dioxo-1,3-dithiane (5)

A solution of 2-*tert*-butyl-1,3-propanedithiol [16] (3.11 g, 18.9 mmol), 4-iodoacetophenone (4.75 g, 18.9 mmol) and *p*-toluenesulphonic acid (0.30 g, 1.6 mmol) in 40 mL acetonitrile was stirred at for 24 h. The solvent was removed under reduced pressure and the residue was partitioned between water and CH_2Cl_2 three times. The organic layers were combined, dried with anhydrous Na_2SO_4 and salts filtered off. The mixture was eluted through a short silica gel column using hexanes to give a mixture of the *cis/trans* isomers of **3** (7.20 g, 18.4 mmol) as a white solid [11]. This mixture was then dissolved in 40 mL CH_2Cl_2 and a solution of MCPBA (3.49 g, 20.2 mmol) in 20 mL CH_2Cl_2 was added slowly at 0°C and then warmed up to 25°C and stirred for 24 h. The mixture was then partitioned between water and CH_2Cl_2 three times. The organic layers were combined, dried with anhydrous Na_2SO_4 and salts filtered off. The filtrate was concentrated under reduced pressure and loaded to a short silica gel column. The column was washed with 25% EtOAc in hexanes to remove the excess of starting material. The product was washed off with 50% EtOAc in hexanes and the eluent evaporated to give a mixture containing all possible isomers of monoxides **4** (5.78 g, 15.6 mmol, 85%) as a white solid. The product mixture was dissolved in 120 mL anhydrous acetone containing $KMnO_4$ (7.83 g, 49.5 mmol), 2 g anhydrous $MgSO_4$ and stirred at for 4 h. The mixture was then filtered through a short florisil column before running a column chromatography with 10% EtOAc in hexanes. *Cis*-**5** (4.37 g, 10.3 mmol, 66%) and *trans*-**5** (1.39 g, 3.28 mmol, 21%) were obtained as white solids. Characterization data: *cis*-**5** m.p. 163–164°C. ^{1}H NMR ($CDCl_3$, 300 MHz) □ 0.88 (s, 9H), 1.84 (s, 3H), 2.52~2.75 (m, 4H), 3.00~3.07 (m, 1H), 7.77 (d, J = 8.4 Hz, 2H), 7.86 (d, J = 8.4 Hz, 2H). MS(ESI+): 447 $[M+Na]^+$, 479 $[M+Na+MeOH]^+$, 871 $[2M+Na]^+$, 1295 $[3M+Na]^+$. HRMS(ESI+): $[M+Na+MeOH]^+$ Calc.: 479.0188; Found: 479.0190; *trans*-**5** m.p. 172–173°C. ^{1}H NMR ($CDCl_3$, 300 MHz) _ 1.02 (s, 9H), 2.23 (s, 3H), 2.59 (tt, J = 11.1 Hz, 2.4 Hz, 1H), 2.82 (dd, J = 14.1Hz, 2.4 Hz, 1H), 2.97 (dd, J = 14.1Hz, 11.1 Hz, 1H), 3.11 (dd, J = 14.1Hz, 11.1 Hz, 1H), 3.25 (dd, J = 14.1Hz, 2.4 Hz, 1H), 7.54 (d, J = 8.4 Hz, 2H), 7.77 (d, J = 8.4 Hz, 2H). MS(ESI+): 447 $[M+Na]^+$, 479 $[M+Na+MeOH]^+$, 871 $[2M+Na]^+$, 1295 $[3M+Na]^+$. HRMS(ESI+): $[M+Na+MeOH]^+$ Calc.: 479.0188; Found: 479.0177.

2.3. trans-5-*tert*-Butyl-2-(4′-(3-hydroxypropynyl)-phenyl)-2-methyl-1,1-dioxo-1,3-dithiane (6)

To a suspension of *trans*-**5** (1.82 g, 42.8 mmol) in 40 mL Et_3N containing 100 mg (PPh_3) $PdCl_2$ and 150 mg CuI, was added propargyl alcohol (1.27 mL, 212 mmol). The mixture was stirred at r.t. overnight. The mixture was filtered and washed with ether. The filtrate was

concentrated under reduced pressure to give a brown solid. Column chromatography with 50% EtOAc in hexanes gave **6** (1.33 g, 37.7 mmol, 88%) as a yellowish solid. m.p. 185–186° C. ^{1}H NMR (Acetone-d_6, 300 MHz) □ 1.06 (s, 9H), 2.28 (s, 3H), 2.50 (tt, J = 11.1 Hz, 2.4 Hz, 1H), 2.90~2.30 (m, 1H), 3.12~3.25 (m, 2H), 3.37 (dd, J = 14.1Hz, 11.1 Hz, 1H), 4.40–4.55 (br, 3H), 7.47 (d, J = 8.4 Hz, 2H), 7.80 (d, J = 8.4 Hz, 2H). MS(ESI+): 375 $[M+Na]^+$, 407 $[M+Na+MeOH]^+$, 727 $[2M+Na]^+$, 1079 $[3M+Na]^+$. HRMS(ESI+): $[M+Na]^+$ Calc.: 375.1065; Found: 375.1060.

2.4. trans-5-*tert*-Butyl-2-(4′-(3-tosyloxypropynyl)-phenyl)-2-methyl-1,1-dioxo-1,3-dithiane (7)

A solution of **6** (0.76 g, 2.16 mmol), *p*-toluenesulfonyl chloride (1.03 g, 5.39 mmol), DMAP (53 mg, 0.43 mmol) and diisopropylethylamine (0.75 mL, 4.3 mmol) in 40 mL CH_2Cl_2 was stirred at 0°C for 3 h. The solvent was removed under reduced pressure and the residue was loaded onto a silica column. Eluating the column with 25% EtOAc in hexanes gave **7** (0.49 g, 0.97 mmol, 45%) as a white solid. m.p. 170–171°C. ^{1}H NMR ($CDCl_3$, 300 MHz) □ 1.01 (s, 9H), 2.23 (s, 3H), 2.38 (s, 3H), 2.58 (tt, J = 11.1 Hz, 2.4 Hz, 1H), 2.82 (dd, J = 14.1Hz, 2.4 Hz, 1H), 2.96 (dd, J = 14.1Hz, 11.1 Hz, 1H), 3.11 (dd, J = 14.1Hz, 11.1 Hz, 1H), 3.23 (dd, J = 14.1Hz, 2.4 Hz, 1H), 4.96 (s, 2H), 7.28 (d, J = 8.4 Hz, 2H), 7.31 (d, J = 8.4 Hz, 2H), 7.72 (d, J = 8.4 Hz, 2H), 7.85 (d, J = 8.4 Hz, 2H). MS(ESI+): 529 $[M+Na]^+$, 1035 $[2M+Na]^+$, 1541 $[3M+Na]^+$. HRMS(ESI+): $[M+Na]^+$ Calc.: 529.1153; Found: 529.1151.

2.5. trans-5-*tert*-Butyl-2-(4′-fluoropropynylphenyl)-2-methyl-1,1-dioxo-1,3-dithiane (1)

A solution of **7** (50 mg, 0.10 mmol), KF (12 mg, 0.21 mmol), and 18-crown-6 (52 mg, 0.20 mmol) in 3 mL anhydrous DMF was stirred at 110°C for 16 h. The solvent was removed under reduced pressure and the residue was loaded onto a silica column. Eluting the column with 10% EtOAc in hexanes gave **1** (9.5 mg, 0.03 mmol, 27%) as a white solid. m.p. 139–141° C. ^{1}H NMR ($CDCl_3$, 300 MHz) δ 1.02 (s, 9H), 2.26 (s, 3H), 2.59 (tt, J = 11.1 Hz, 2.4 Hz, 1H), 2.83 (dd, J = 13.1Hz, 2.4 Hz, 1H), 2.98 (dd, J = 13.1 Hz, 11.1 Hz, 1H), 3.13 (dd, J = 13.1 Hz, 11.1 Hz, 1H), 3.25 (dd, J = 13.1 Hz, 2.4 Hz, 1H), 5.17 (d, J = 47.5 Hz, 2H), 7.52 (d, J = 8.4 Hz, 2H), 7.79 (d, J = 8.4 Hz, 2H). MS(ESI+): 377 $[M+Na]^+$, 409 $[M+Na+MeOH]^+$, 731 $[2M+Na]^+$, 1085 $[3M+Na]^+$. HRMS(ESI+): $[M+Na]^+$ Calc.: 377.1021; Found: 377.1022.

2.6. trans-5-*tert*-Butyl-2-(4′-[^{18}F]fluoropropynylphenyl)-2-methyl-1,1-dioxo-1,3-dithiane ([^{18}F] 1)

A solution of *c.a*. 2 mg **7** and no-carrier-added [^{18}F]KF prepared as described earlier in 200 □L anhydrous DMF was sealed in a 4 mL V-vial and heated at 85°C for 20 min. The crude mixture was loaded onto a reverse phase HPLC column (Phenomenex Synergi Max-RP 4□, 50 × 4.6 mm, 2 mL/min.) and eluted with 40% EtOH/H_2O. The radioactive peak was collected (t_R=7.0 min) and solvent was evaporated with heat. The remaining product was formulated as a 100 □Ci/mL saline solution. Quality control was performed with both TLC analysis (50% ethyl acetate in hexanes as the developing eluent, R_f = 0.6) and HPLC analysis with the same system as the preparative procedure. The radiochemical yield was 12–27% (decay-corrected) with >95% radiochemical purity and >1000 Ci/mmol specific activity.

2.7. cis-/trans-5-*tert*-Butyl-2-(4′-(3-tosyloxypropynyl)-phenyl)-2-methyl-1,1,3,3-tetraoxo-1,3-dithiane(*cis-/trans*-9)

To a solution of 2-*tert*-butyl-1,3-propanedithiol (0.60 g, 3.67 mmol), 1-tosyl-3-(4′-acetylphenyl)-2-propyne [17] (1.21 g, 3.67 mmol) in CH_2Cl_2 was added BF_3-Et_2O (0.14 mL, 1.10 mmol) dropwise at 0°C. The mixture was kept at 0°C for 2 hr. and then allowed to warm up to r.t. and stirred overnight. The reaction was then quenched with saturated $NaHCO_3$ aqueous solution and partitioned between water and CH_2Cl_2 three times. The organic layers were combined, dried with anhydrous Na_2SO_4 and salts filtered off. The mixture was run

through a short silica gel column with 10% ethyl acetate in hexanes to give a mixture of the *cis/trans* isomers of **8** (1.59 g, 3.34 mmol, 91%) as an oil. This mixture was then dissolved in 40 mL CH_2Cl_2 and a solution of MCPBA (2.88 g, 16.7 mmol) in 20 mL CH_2Cl_2 was added slowly at 0°C and then warmed up to r.t. and stirred overnight. The mixture was then partitioned between aqueous $NaHCO_3$ solution and CH_2Cl_2 three times. The organic layers were combined, dried with anhydrous Na_2SO_4 and salts filtered off. The filtrate was concentrated under reduced pressure, and column chromatography with 30% ethyl acetate in hexanes gave the *cis*-**9** (0.75 g, 1.40 mmol, 42%) and *trans*-**9** (0.51 g, 0.94 mmol, 28%) as white solids. Characterization data: *cis*-**9** m.p. 155°C with decomposition. ^{1}H NMR ($CDCl_3$, 300 MHz) □ 1.01 (s, 9H), 2.21 (s, 3H), 2.41 (s, 3H), 2.56 (tt, *J* = 12.4 Hz, 2.4 Hz, 1H), 3.20 (dd, *J* = 14.8 Hz, 12.4 Hz, 2H), 3.42 (dd, *J* = 14.8 Hz, 2.4 Hz, 2H), 4.94 (s, 2H), 7.34 (d, *J* = 8.4 Hz, 2H), 7.36 (d, *J* = 8.4 Hz, 2H), 7.73 (d, *J* = 8.4 Hz, 2H), 7.85 (d, *J* = 8.4 Hz, 2H). MS(ESI+): 561 [M +Na]$^+$. HRMS(EI+): [M]$^+$ Calc.: 538.1154; Found: 538.1156; *trans*-**9** m.p. 181°C with decomposition. ^{1}H NMR ($CDCl_3$, 300 MHz) δ 1.07 (s, 9H), 2.31 (s, 3H), 2.38 (s, 3H), 2.65 (m, 1H), 3.35 (m, 4H), 4.97 (s, 2H), 7.31 (d, *J* = 8.4 Hz, 4H), 7.85 (d, *J* = 8.4 Hz, 2H), 7.95 (d, *J* = 8.4 Hz, 2H). MS(ESI+): 561 [M+Na]$^+$, 1099 [2M+Na]$^+$. HRMS(EI+): [M]$^+$ Calc.: 538.1154; Found: 538.1145.

2.8. trans-5-*tert*-Butyl-2-(4′-fluoropropynylphenyl)-2-methy-1,1,3,3-tetraoxo-1,3-dithiane (*trans*-2)

A solution of *trans*-**9** (50 mg, 0.09 mmol), KF (11 mg, 0.19 mmol), and 18-crown-6 (52 mg, 0.20 mmol) in 3 mL anhydrous DMF was stirred at 110°C for 16 h. The solvent was removed under reduced pressure and the residue was loaded onto a silica column. Eluting the column with 25% EtOAc in hexanes gave **2** (10 mg, 0.03 mmol, 30%) as a white solid. m.p. 264°C with decomposition. ^{1}H NMR ($CDCl_3$, 300 MHz) δ 1.13 (s, 9H), 2.39 (s, 3H), 2.55 (tt, *J* = 12.6 Hz, 2.4 Hz, 1H), 3.50 (dd, *J* = 13.1 Hz, 2.4 Hz, 2H), 3.79 (m, *J* = 13.1Hz, 12.6 Hz, 2H), 5.32 (d, *J* = 47.2 Hz, 2H), 7.60 (d, *J* = 8.7 Hz, 2H), 8.14 (d, *J* = 8.7 Hz, 2H). MS(ESI+): 409 [M +Na]$^+$, 441 [M+Na+MeOH]$^+$, 795 [2M+Na]$^+$. HRMS(EI+): [M]$^+$ Calc.: 386.1022; Found: 386.1017.

2.9. trans-5-*tert*-Butyl-2-(4′-[^{18}F]fluoropropynylphen-yl)-2-methyl-1,1,3,3-tetraoxo-1,3-dithiane(*trans*-[^{18}F]2)

Trans-[^{18}F]**2** was synthesized using the same procedure as the preparation of [^{18}F]**1** except that *trans*-**9** was used as precursors. The crude mixture was purified with a reverse phase HPLC column (Phenomenex Primesphere 5□ C8, 30 × 4.6 mm, 2 mL/min.) and eluted with 30% EtOH/H_2O. The radioactive peak was collected (t_R=7.5 min) and solvent was evaporated with heat. The remaining product was formulated as a 100 □Ci/mL saline solution. Quality controls were performed with both TLC analysis (50% ethyl acetate in hexanes as the developing eluent, R_f = 0.6 for *trans*-[^{18}F]**2**) and HPLC analysis with the same system as the preparative procedure. The radiochemical yield was 7–35% (decay-corrected) with >96% radiochemical purity and >1000 Ci/mmol specific activity.

2.10. In Vitro Radioligands Competition Studies

Binding assays employed tissue homogenates obtained from the cerebral cortices of adult male Sprague-Dawley rats. Briefly, cerebral cortex was dissected and homogenized in cold phosphate-buffered saline (PBS: NaCl, 124 mM; KCl, 2.7 mM; Na_2HPO_4, 7.7 mM; KH_2PO_4, 1.5 mM; pH 7.4 at 37°C). After centrifugation at 10,000 × g for 20 min, the pellet was twice resuspended and recentrifuged to remove as much endogenous GABA as possible. The tissue preparation was stored at −70°C until use in binding assays. Assays were conducted in triplicate, employing 0.2 mg protein in 1 mL of PBS for each measurement. The radioligand 4′-ethynyl-4-n-[2,3-$^3H_2$]propylbicycloorthobenzoate ([3H]EBOB; New England Nuclear,

Boston, MA; specific activity 30 mCi/mmol) at a final concentration of 5 nM was used to radiolabel the $GABA_A$ ionophore binding site as described previously [18–21]. Unlabeled ligands under investigation were added to achieve final concentrations ranging from 0.01 nM to 100 nM. Assays were incubated for 1 hour at 37°C followed by rapid filtration over glass-microfiber filters (Whatman GF/C filters, pretreated with 0.1% polyethylenimine in PBS). Filters were washed sequentially with 3 × 2 mL aliquots of PBS and were then assessed by liquid scintillation spectroscopy. Non-saturable binding was defined in the presence of 100 μM picrotoxin (Sigma, St. Louis, MO).

2.11. In Vivo Biodistribution Studies in Mouse Brain

Female CD-1 mice were anesthetized with diethyl ether and 10–15 μCi of *trans*-[^{18}F]**1** or *trans*-[^{18}F]**2** formulated as a saline solution were injected *via* the tail vein. At different time points (2 min to 2 h) after the injections, groups of animals (n=4) were sacrificed by decapitation, and the brains were rapidly removed and dissected into samples of striatum, cortex, hippocampus, cerebellum, pons-medulla, and the remainder of the brain. Tissue samples were weighed and counted in an automatic γ-counter. The amount of radioactivity in each brain region was calculated as percent injected dose/gram of tissue (%ID/g).

3. Results

3.1. Chemistry

The syntheses of the dithianes and S-oxide products (compounds **1** and **2** as well as the other dithianes in Table 1) followed the methods of Casida and co-workers [9,10,13–15]. Although a published synthetic sequence, the preparation of these dithiane oxides required careful attention to separation of isomers and identification of sulfur oxidation states. The key to control the oxidation states of the sulfur atoms was the selective oxidation with *m*-chloroperbenzoic acid (MCPBA) or potassium permanganate. The stereochemical configuration of the dithianes was assigned by NMR analysis according to literature methods [10].

The syntheses of compound **1** in fluorine-19 and fluorine-18 forms are outlined in Scheme 1. Condensation of 2-*tert*-butyl-1,3-propanedithiol [16] with 4-iodoacetophenone in acetonitrile in the presence of *p*-toluenesulfonic acid yielded a mixture of *cis*- and *trans*-5-*tert*-butyl-2-(4′-iodophenyl)-2-methyl-1,3-dithiane **3** in 97% yield. The mixture was mono-oxidized by treating with 1 equivalent of *m*-chloroperoxybenzoic acid (MCPBA) in dichloromethane at low temperature. The newly introduced S=O bond could take either the axial or the equatorial conformation; all the four possible diastereomers (with respect to *cis/trans* configuration at the carbon atom center as well as equatorial *vs*. axial S-oxidation) of **4** were observed by careful NMR analysis. This mixture of isomers of **4** was then oxidized with potassium permanganate to give a mixture of *cis*- and *trans*-5-*tert*-butyl-2-(4′-iodophenyl)-2-methyl-1,1-dioxo-1,3-dithiane **5** in high yield. At this point in the synthesis the two isomers *cis*-**5** and *trans*-**5** were isolated easily with column chromatography. The overall yield of the desired *trans*-**5** was 24% starting from 2-*tert*-butyl-1,3-propanedithiol. The ethynyl group was introduced by coupling *trans*-**5** with propargyl alcohol in the presence of palladium catalyst [14]. The resulting alcohol **6** was treated with tosyl chloride to yield **7** as the precursor for fluorine substitution, and a small amount of compound **7** was converted to *trans*-5-*tert*-butyl-2-(4′-fluoropropynylphenyl)-2-methyl-1,1-dioxo-1,3-dithiane **1** with potassium fluoride and 18-crown-6 as a phase-transfer catalyst in dimethylformamide.

The synthesis of *trans*-5-*tert*-butyl-2-(4′-fluoropropynylphenyl)-2-methyl-1,1,3,3-tetroxo-1,3-dithiane **2** was considerably simpler. As illustrated in Scheme 2, 2-*tert*-butyl-1,3-propanedithiol was coupled with 4′-(3-tosyloxypropynyl)acetophenone [17], and the resulting

cis-/*trans*- mixture of dithianes **8** (which could not be separated by column chromatography) was treated with excess MCPBA to fully oxidize the molecules to *cis*- and *trans*-dithiane tetraoxides **9**. The stereoisomers were at this stage easily resolved using simple column chromatography. An authentic sample of *trans*-**2** was prepared as described above using KF/18-crown-6 in dimethylformamide.

For both radioligands, incorporation of fluorine-18 was then done at the last step in reasonable radiochemical yields (7–35% decay-corrected), in reaction times of one hour including purification, and specific activities >1000 Ci/mmol. Parameters for radiolabeling were not optimized.

3.2. Biology

3.2.1. *In Vitro* Radioligand Competition Analysis—The unlabeled compounds 1 and *trans*-2 were evaluated for their ability to compete with [^{3}H]EBOB binding in rat brain cortex P3 fractions. The K_i values for compounds *trans*-**1** and *trans*-**2** were both determined to be 6.5 nM (Table 1).

3.2.2. *In Vivo* Biodistribution Studies in Mouse Brain—Radioligand [^{18}F]**1** showed high initial uptake into mouse brain after intravenous injection, followed by a continuous washout up to 60 minutes (Table 2). At 30–60 minutes post-injection, there was a clear heterogeneous regional brain distribution with higher retention in cerebral cortex and cerebellum and lower in striatum and pons-medulla. *Trans*-[^{18}F]**2** showed an equivalent initial uptake (Table 3), slower clearance from the brain tissues and similar heterogeneity of regional distribution at the later time points.

4. Discussion

The dithiane oxides **1** and **2** were chosen for radiolabeling based on the following characteristics. First, they had the highest in vitro binding affinity for the GABA-ionophore binding site (6.5 nM) of a series of compounds prepared in our laboratories, as measured using a consistent in vitro assay of competition for the binding of the radioligand [^{3}H]EBOB (Table 1). Our results are similar to the data of Wacher *et. al*. [10] who reported equivalent binding affinities for the di-, tri-, and tetraoxides of 5-*tert*-butyl-2-(4′-ethynylphenyl)-1,3-dithiane. Second, labeling with fluorine-18 could be done in the last step of the synthesis by nucleophilic displacement of a tosyloxy leaving group, with the potential side reaction of epimerization at the acidic benzylic carbon blocked with the 2-methyl substituent. Finally, as oxidation of the sulfur atoms has been reported as a primary route of in vivo metabolism for these dithianes [22], the use of the oxidized species as the radioligands would reduce or eliminate (in the case of the tetraoxo derivative) the number of potential in vivo metabolites.

Initial evaluation of these two radioligands was done in the mouse brain, as this provides a convenient and rapid screen of a new radioligand. Early studies of a new radioligand most often are meant to address several key features of successful radioligands for imaging of high affinity sites (receptors, transporters, enzymes) in the brain: adequate penetration of the blood-brain-barrier, a reasonable egress of unbound radioactivity from the brain, and selective retention of radioactivity in regions of high concentrations of targeted binding sites. Only when encouraging results are obtained in the initial studies does the testing progress to the next steps of evaluation of the regional brain distribution in a model of pharmacological challenge (blocking studies) or in a transgenic (knockout) animal to demonstrate specificity of binding, and metabolism studies to verify identity of radioactivity in the brain tissues.

For the two new $GABA_A$ receptor-targeting radioligands [^{18}F]**1** and [^{18}F]**2**, the most optimistic view was that these new compounds met these initial qualifications, and deserved further

evaluation as potential in vivo radioligands for the $GABA_A$ receptor. Despite the relatively high molecular weight for these molecules, brain uptake at an early (2 min) time point was quite reasonable (>4% ID/g), similar to what we have obtained with highly successful radioligands such as [^{11}C]carfentanil (3.6 %ID/g). The pharmacokinetics of unbound radioligand, which would define the level of residual non-specific binding at later time points, also is reasonable as significant washout of radioactivity from the pons (>50%) is observed over the first hour after injection for both compounds. Finally, one can construct correlations between regional brain uptake of these compounds and both in vitro measures of radioligand binding to sites on the $GABA_A$ receptor complex. For example, the distribution of these new radioligands correlates (r = 0.94, Fig. 1A) with the distribution of in vitro binding sites for [^{3}H]TBOB in the rat brain, with the expected rank order of cortex > cerebellum > striatum > pons [23], (unfortunately, corresponding data for the mouse brain in unavailable). The in vivo distribution of these fluorine-18 labeled dithiane oxides also correlates (r = 0.97, Fig. 1B) with the rank order of regional distribution of the benzodiazepine [^{11}C]flumazenil in mouse brain with the exception of the cerebellum; whereas there are high levels of binding of specific radioligands to the GABA-ionophore binding site in the cerebellum, the subunit composition of many cerebellar $GABA_A$ receptors does not include the flumazenil binding site [24]. Of the ten 5-*tert*-butyl-2-phenyl-1,3-dithianes and corresponding oxides labeled to date with fluorine-18, carbon-11 or iodine-125, *trans*-[^{18}F]**1** and *trans*-[^{18}F]**2** have clearly shown the most persistent brain retention and better regional heterogeneity. Thus, an optimistic view is that these new radioligands show good brain uptake, show egress of unbound activity from the brain, and present a heterogeneous brain distribution that correlates with the distribution of the targeted $GABA_A$ receptor.

Will these new radioligands [^{18}F]**1** and [^{18}F]**2** succeed as imaging agents sensitive enough to quantify physiologically relevant changes in the GABA receptor ionophore-binding site in a disease state, or measure changes in response to drug challenges? The dynamic range for the purported specific binding, as measured using maximal target-to-nontarget ratios (CBL/PONS or CTX/PONS) never exceeded a value of two. One reasonable question at this point was whether the low specific binding ratios (<2) were due to poor affinity for the receptor, poor pharmacokinetics (too fast or too slow for dissociation from binding site), or high non-specific retention of unbound radioactivity. These are in fact the very first questions asked when any first in vivo experiments with a new radiotracer fail to provide evidence for clear and easily recognized specific binding in the brain. Fortunately, as part of the comprehensive program in PET radioligand development in our institution, we have extensive prior experience in just this area. In Table 4 are shown the regional brain concentrations for in vivo studies of more than two dozen different potential radioligands, targeting nine different neurochemical targets (receptors, transporters and enzymes). All of these studies were done using ex vivo tissue dissection and counting, and all were done by the identical protocol in CD-1 mice. Comparison of the in vivo distribution of the new radioligands [^{18}F]**1** and [^{18}F]**2** with this series of dissimilar radiotracers provides some insight into likely shortcomings of the new compounds. The residual radioactivity in non-target regions (e.g., pons) for the new radioligands [^{18}F]**1** and [^{18}F]**2** is similar or even lower than the majority of other radioligands, some of which have proven to be eventually useful in successful clinical studies (e.g., [^{11}C]flumazenil, [^{11}C] carfentanil, [^{11}C]NMPB, [^{11}C]DTBZ). This suggests that it is not simply high non-specific distribution of radioactivity (authentic radiotracer or metabolites) which is responsible for the lower target-to-nontarget ratios (<2) observed for [^{18}F]**1** and [^{18}F]**2**. In contrast, the data in Table 4 shows that uniformly there was higher retention of radioactivity in target regions for the truly successful radioligands. In other words, for the successful radiotracers in Table 4, obtaining encouraging tissue concentration ratios (an early indicator of specific binding provided by this simple mouse model) was more likely due to retention of radioligand in the target region rather than complete washout of nonspecific binding. As most investigators equate retention of radioactivity with affinity of the radioligand for the target protein, these

data would support a conclusion that higher affinity derivatives related to [^{18}F]**1** and [^{18}F]**2** might provide higher retention in the cortex and lead to improved cortex/pons ratios.

The simple expectation that higher affinity radioligands would automatically lead to drastically improved tissue ratios also needs to be more closely examined. A first question is whether there are sufficient binding sites available, such that specific binding might be expected for radioligands with low nanomolar (<10) affinities such as attained by [^{18}F]**1** and [^{18}F]**2.** This would appear not to be the problem, as the concentration (B_{max}) of binding sites for radioligands such as [3H]TBOB and [^{3}H]EBOB in vitro are 1000–2000 fmol/mg protein in the cortex [23,25]; estimating the target/nontarget ratio as the value B_{max}/K_d would support acceptable results might be attainable with the new radioligands [^{18}F]**1** and [^{18}F]**2** (if B_{max} = 2000 fmol/mg protein, K_d approx. 6–10 nM, B_{max}/K_d = 20–33) [25]. The difficulty in the GABA receptor system is that the in vitro radioligand binding data for the GABA-ionophore-binding site in the rat brain shows that the dynamic range of site concentrations may in fact be inherently quite small (in vitro cortex/pons < 4), which is an order of magnitude less than the in vitro tissue ratios achievable with such ligands as those for the VMAT2 site in the striatum (in vitro values: caudate-putamen 1190 ± 180 and cerebellum 60 ± 12 fmol/mg protein, striatum/cerebellum = 60 [26]). It should be noted that the in vitro STR/CBL value of 60 for VMAT2 radioligand binding translates to a distribution volume ratio (DVR) value of only 3.62 ± 0.35 for an in vivo equilibrium model of rat brain binding of the highly specific radioligand (+)-[^{11}C]dihydrotetrabenazine [27]. So it remains conceivable that modest tissue concentration ratios, such as obtained here with [^{18}F]**1** and [^{18}F]**2**, are more to be expected with radioligands for the GABA-ionophore-binding site than with some of the other neurochemical systems previously targeted for radiotracer development for in vivo imaging.

As the $GABA_A$ receptor is widespread throughout the brain and of fundamental importance to brain function, further development of radioligands for the GABA-ionophore-binding remains of interest but is also significantly challenging. The demonstration of specificity of binding, either for compound [^{18}F]**1** and [^{18}F]**2** or perhaps yet to be discovered higher affinity radioligands, is difficult as traditional pharmacological blocking studies are ruled out due to the pharmacological toxicity (seizures) induced by administration of picrotoxin and related pharmacological agents. Validation studies may very well require use of selective knockout models with reduced binding site concentrations [4]. Studies of the $GABA_A$ receptor are also complicated by effects of anesthesia, as it is quite clear that some anesthetic agents (volatile anesthetics such as isoflurane) have specific binding sites on the receptor complex [1]. Finally, the $GABA_A$ receptor is one of the most complex in the brain with multiple binding sites for agonists and antagonists (which can vary regionally in the brain), and the binding of radioligands to the ionophore (picrotoxin) site can be modulated by binding of ligands to these other sites [24]. These reasons, along with the fundamental questions raised earlier of whether high binding ratios are truly achievable in this system, make further study of radioligands for the ionophore-binding site of the $GABA_A$ receptor perhaps more difficult than some of the other neurochemical systems in the brain.

Conclusion

We have reported the synthesis and initial in vivo evaluation of two new high-affinity radioligands for $GABA_A$ receptors. The *trans*-5-*tert*-butyl-2-(4′-fluoropropynylphenyl)-2-methyl-1,1-dioxo-1,3-dithiane **1** and *trans*-5-*tert*-butyl-2-(4′-fluoropropynylphenyl)-2-methyl-1,1,3,3-tetraoxo-1,3-dithiane **2** are high affinity (6.5 nM) radioligands for the ionophore (picrotoxin) site of the $GABA_A$ receptor, demonstrate reasonable initial in vivo brain uptakes, and present heterogeneous distributions at later time points that are consistent with the distribution of the $GABA_A$ receptors. Further evaluation of the in vivo pharmacokinetics, pharmacological specificity, and metabolism of these radioligands is warranted, but a

continued effort to discover even higher affinity ligands with potential for radiolabeling with positron-emitting radionuclides such as carbon-11 and fluorine-18 may prove more successful at development of a PET radiopharmaceutical for human PET imaging.

Acknowledgements

This work was supported by grant NS-15655 from the National Institutes of Health. The authors thank the cyclotron staff of the University of Michigan Cyclotron/PET facility for radionuclide production.

References

1. Johnston GAR. $GABA_A$ receptor channel pharmacology. Current Pharm Design 2005;11:1867–1885.
2. Krogsgaard-Larsen, Frølund P, Jørgensen B, Schousboe FS. A $GABA_A$ receptor agonists, partial agonists, and antagonists. Design and therapeutic prospects. J Med Chem 1994;37:2489–2505. [PubMed: 8057295]
3. Burt DR. Reducing GABA receptors. Life Sci 2003;73:1741–1758. [PubMed: 12888114]
4. Korpi ER, Gründer G, Lüddens H. Drug interactions at $GABA_A$ receptors. Prog Neurobio 2002;67:113–159.
5. Katsifis A, Kassiou M. Development of radioligands for in vivo imaging of GABA(A)-benzodiazepine receptors. Mini-Reviews Med Chem 2004;4:909–21.
6. Chen L, Durkin KA, Casida JE. Structural model for g-aminobutyric acid receptor noncompetitive antagonist binding; Widely diverse structures fit the same site. Proc Natl Acad Sci 2006;103:5185–5190. [PubMed: 16537435]
7. Mulholland GK, Kilbourn MR. [^{18}F]Fluoro-tert-butyl-bicycloorthobenzoate (FTBOB): a potetntial tracer for the GABAA chloride channel. J Label Compd Radiopharm 1993;32:313.
8. Culbert PA, Chan S, Wearring AV, Chamberlain MJ, Hunter DH. Potential imaging agent for the $GABA_A$ receptor: 4-t-butyl-1-(4-[^{123}I]iodophenyl)-2,6,7-trioxabicyclo-[2.2.2]octane. Nucl Med Biol 199;20:469–475. [PubMed: 8389222]
9. Elliot M, Pullman DA, Larkin JP, Casida JE. Insecticidal 1,3-dithianes. J Agric Food Chem 1992;40:147–151.
10. Wacher VJ, Toia RE, Casida JE. 2-Aryl-5-tert-butyl-1,3-dithianes and their S-oxidation products: Structure-activity relationships of potent insecticides acting at the GABA-gated chloride channel. J Agric Food Chem 1992;40:497–505.
11. Snyder SE, Kume A, Jung Y-W, Conner SE, Sherman PS, Albin RL, Wieland DM, Kilbourn MR. Synthesis of carbon-11, fluorine-18 and iodine-125 labeled GABAA-gated chloride ion channel blockers: substituted 5-t-butyl-2-phenyl-1,3-dithianes and dithiane oxides. J Med Chem 1995;38:2663–2671. [PubMed: 7629805]
12. Blair JB, Snyder SE, Sherman PS, Kilbourn MR. Synthesis and in vivo characterization of substituted 5-tert-butyl-2-phenyl-2-[^{11}C]methyldithiane oxides as potential PET imaging agents for the $GABA_A$ chloride ion channel. J Label Compd Radiopharm 1999;42(Suppl 1):S635–S637.
13. Palmer CJ, Casida JE. Insecticidal 1,3-dithianes and 1,3-dithiane 1,1-dioxides. J Agric Food Chem 1992;40:492–496.
14. Li QX, Casida JE. Structure-activity studies leading to potent chloride channel blockers: 5e-tert-Butyl-2-[4-(substituted-ethynyl)phenyl]-1,3-dithianes. Bioorg Med Chem 1994;2:1423–1434. [PubMed: 7788306]
15. Li QX, Casida JE. Affinity probes for the GABA-gated chloride channel: 5e-tert-butyl-2e-[4-(substituted-ethynyl)phenyl]-1,3-dithianes with photoactivatable, fluorescent, biotin, agarose and protein substituents. Bioorg Med Chem 1995;3:1675–1684. [PubMed: 8770392]
16. Eliel EL, Rao V, Smith S, Hutchins RO. Convenient and stereoselective dithiol synthesis. J Org Chem 1975;40:524–526.
17. Scott EE, Donnelly ET, Welker ME. Preparation of substituted transition-metal (η^1-propargyl complexes and their [3+2] cycloaddition reactions with sulfur dioxide and disulfur monoxide. Transition-metal–carbon bond cleaving reactions of the cycloadducts which yield oxathiolene oxides and dithiolene oxides. J Organometal Chem 2003;673:67–76.

18. Huang J, Casida JE. Characterization of [^{3}H]ethynylbicycloorthobenzoate ([^{3}H]EBOB) binding and the action of insecticides on the gamma-aminobutyric acid-gated chloride channel in cultured cerebellar granule neurons. J Pharmacol Exp Ther 1996 Dec;279(3):1191–6. [PubMed: 8968340]
19. Huang J, Casida JE. Role of cerebellar granule cell-specific $GABA_A$ receptor subtype in the differential sensitivity of [^{3}H]ethynylbicycloorthobenzoate binding to GABA mimetics. Neurosci Lett 1997 Apr 4;225(2):85–8. [PubMed: 9147380]
20. Nicholson RA, Lees G, Zheng J, Verdon B. Inhibition of GABA-gated chloride channels by 12,14-dichlorodehydroabietic acid in mammalian brain. Br J Pharmacol 1999 Mar;126(5):1123–32. [PubMed: 10204999]
21. Kume A, Albin RL. Quantitative autoradiography of 4′-ethynyl-4-n-[2,3-$^{3}H_2$] propylbicycloorthobenzoate binding to the $GABA_A$ receptor complex. Eur J Pharmcol 1994;263:163–173.
22. Wacher VJ, Casida JE. Metabolism in mouse liver and photooxidation of the insecticidal cis and trans-2-(4-bromophenyl)-5-tert-butyl-1,3-dithianes. J Agri Food Chem 1993;41:296–302.
23. Lawrence LJ, Palmer CJ, Gee KW, Wang X, Yumamura HI, Casida JE. t[^{3}H] Butylbicycloorthobenzoate: New radioligand probe for the γγ-aminobutyric acid–regulated chloride ionophore. J Neurochem 1985;45:798–804. [PubMed: 2993514]
24. Olsen RW, McCabe RT, Wamesley JK. GABAA receptor subtypes: Autoradiographic comparison of GABA, benzodiazepine, and convulsant binding sites in the rat central nervous system. J Chem Neuroanat 1990;3:59–76. [PubMed: 2156526]
25. Eckelman WC, Kilbourn MR, Mathis CA. Discussion of targeting protein in vivo: in vitro guidelines. Nucl Med Biol 2006;33:449–451. [PubMed: 16720235]
26. Vander Borght TM, Sima AAF, Kilbourn MR, Desmond TJ, Frey KA. [3H]Methoxytetrabenazine: a high specific activity ligand for estimating monoaminergic neuronal integrity. Neuroscience 1995;68:955–962. [PubMed: 8577387]
27. Kilbourn MR. Long-term reproducibility of in vivo measures of specific binding of radioligands in rat brain. Nucl Med Biol 2004;31:591–595. [PubMed: 15219277]
28. Kilbourn MR, Pavia MR, Gregor VE. Synthesis of fluorine-18 labelled GABA uptake inhibitors. Appl Radiat Isot 1990;41:823–828.
29. Kilbourn MR, Haka MS, Mulholland GK, Sherman PS, Pisani T. Regional brain distribution of [^{18}F]GBR 13119, a dopamine uptake inhibitor, in CD-1 and C57B1/6 mice. Eur J Pharm 1989;166:331–334.
30. Haka MS, Kilbourn MR. Synthesis of [^{18}F]GBR 12909, a dopamine reuptake inhibitor. J Labeled Compds Radiopharm 1990;28:793–800.
31. Haka MS, Kilbourn MR. Synthesis and regional brain distribution of [^{11}C]nisoxetine, a norepinephrine uptake inhibitor. Nucl Med Biol 1989;16:771–774.
32. Mulholland GK, Otto CA, Jewett DM, Kilbourn MR, Koeppe RA, Sherman PS, Petry NA, Carey JA, Atkinson ER, Archer S, Frey KA, Kuhl DE. Synthesis, biodistribution, dosimetry, metabolism and monkey PET studies of carbon-11 labeled (+)-2α-tropanyl benzilate, a central muscarinic receptor imaging agent. J Nucl Med 1992;33:423–430. [PubMed: 1740713]
33. Mulholland GK, Kilbourn MR, Sherman P, Carey JE, Frey KA, Koeppe RA, Kuhl DE. Synthesis, in vivo biodistribution and dosimetry of [11C]N-methylpiperidyl benzilate ([11C]NMPB), a muscarinic acetylcholine receptor antagonist. Nucl Med Biol 1995;22:13–17. [PubMed: 7735163]
34. Skaddan MB, Jewett DM, Sherman PS, Kilbourn MR. (*R*)-*N*-[^{11}C]Methyl-3-pyrrolidinyl benzilate, a high affinity reversible radioligand for PET studies of the muscarinic acetylcholine receptor. Synapse 2002;45:31–37. [PubMed: 12112411]
35. Skaddan MB, Kilbourn MR, Snyder SE, Sherman PS, Desmond TJ, Frey KA. Synthesis, radiolabeling, and biological evalaution of piperidyl and pyrolidyl benzilates as in vivo ligands for the muscarinic acetylcholine receptors. J Med Chem 2000;43:4552–4562. [PubMed: 11087580]
36. Brown-Proctor C, Snyder SE, Sherman PS, Kilbourn MR. Synthesis and *In Vivo* Evaluation of (E)-*N*-[^{11}C]Methyl-4-(3-pyridinyl)-3-butene-1-amine ([^{11}C]Metanicotine) as a Nicotinic Receptor Radioligand. Nucl Med Biol 2000;27:415–418. [PubMed: 10938478]
37. Mulholland GK, Sugimoto H, Jewett DM, Kilbourn MR. Simple preparation of a novel C-11 acetylcholinesterase inhibitor. J Nuc Med 1989;30:822.

38. Brown-Proctor C, Snyder SE, Sherman PS, Kilbourn MR. Synthesis and evaluation of 6-[^{11}C] methoxy-3-[2-[1-(phenylmethyl)-4-piperidinyl]ethyl]-1,2-benzisoxazole as an in vivo radioligand for acetylcholinesterase. Nucl Med Biol 1999;26:99–103. [PubMed: 10096508]
39. Kilbourn MR, Jung Y-W, Haka MS, Gildersleeve DL, Kuhl DE, Wieland DM. Mouse brain distribution of a carbon-11 labeled vesamicol derivative: presynaptic marker of cholinergic neurons. Life Sciences 1990;47:1955–1963. [PubMed: 2266779]
40. Mulholland GK, Jung Y-W, Wieland DM, Kilbourn MR, Kuhl DE. Synthesis of [^{18}F] fluoroethoxybenzovesamicol, a radiotracer for cholinergic neurons. J Labelled Cmpds and Radiopharm 1993;33:583–592.
41. DaSilva JN, Kilbourn MR. In vivo binding of [^{11}C]tetrabenazine to vesicular monoamine transporters in mouse brain. Life Sciences 1992;51:593–600. [PubMed: 1640810]
42. DaSilva JN, Kilbourn MR, Mangner TJ. Synthesis of a [^{11}C]methoxy derivative of α-dihydrotetrabenazine: a radioligand for studying the vesicular monoamine transporter. Appl Radiat Isot 1993;44:1487–1489. [PubMed: 7903060]
43. Kilbourn M, Frey K. Striatal concentrations of vesicular monoamine transporters are identical in MPTP-sensitive (C57Bl/6) and -insensitive (CD-1) mouse strains. Eur J Pharmacol 1996;307:227–232. [PubMed: 8832225]
44. Jewett DM, Kilbourn MR. In vivo evaluation of new carfentanil-based radioligands for the mu opiate receptor. Nucl Med Biol 2004;31:321–325. [PubMed: 15028244]
45. Kilbourn M, Pichika R, Jewett D, Sherman P, Traynor J, Husbands S, Woods J. Synthesis and biodistribution of novel [11C]methyl labeled _-opiod receptor radiotracers. Abstracts of Papers of the American Chemical Society 2001;222(213MEDI Pt 1)

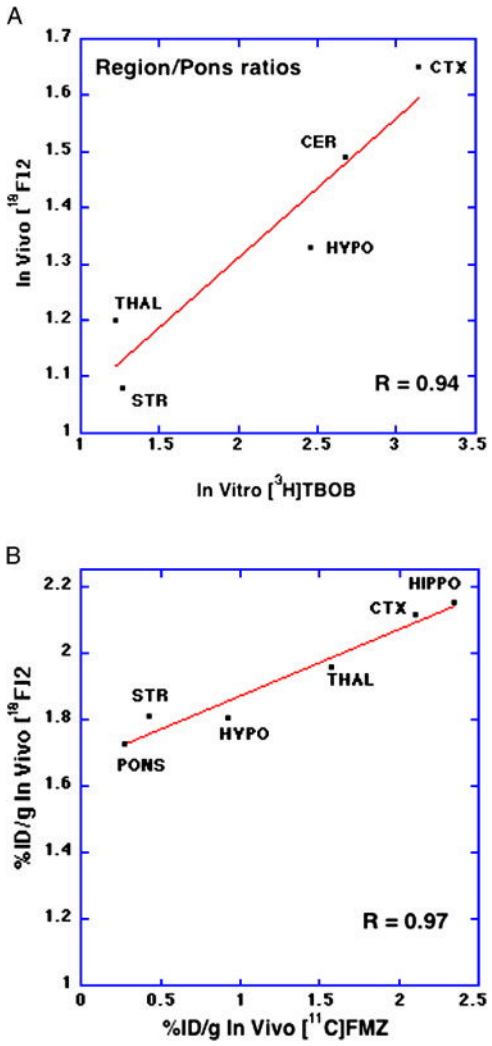

Figure 1.

Figure 1A. Correlation of regional brain tissue ratios for dithiane **2** and in vitro binding of [^{3}H]TBOB in rat brain (data from reference 23). Pons was selected to represent the region of non-specific binding. Abbreviations: str = striatum, thal = thalamus, hypo = hypothalamus, cer = cerebellum, ctx = cortex, hippo = hippocampus.

Figure 1B. Correlation of in vivo regional brain uptake (% injected dose per gram tissue at 30 min) for dithiane **1** and in vivo regional mouse brain distribution of [^{11}C]flumazenil (% injected dose per gram tissue at 45 min: Kilbourn and Sherman, unpublished data). Abbreviations as in Fig 1A.

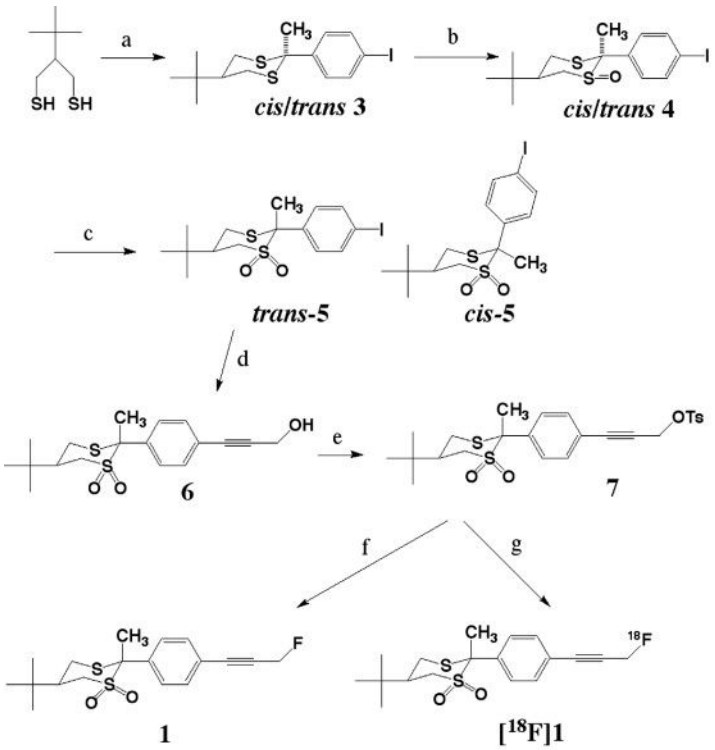

Key: a. 4'-iodoacetophenone, p-TsOH; b. MCPBA, CH_2Cl_2; c, $KMnO_4$,chromatography; d. propargyl alcohol, $Pd(Ph_3P)_2Cl_2$, CuI, Et_3N; e. TsCl, DMAP, iPr_2NEt; f. KF, 18-crown-6; g. [^{18}F]fluoride, K_2CO_3, 18-crown-6

Scheme 1.

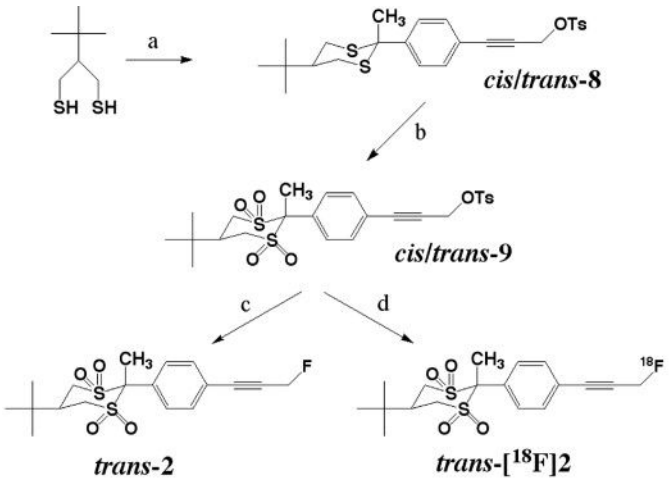

Key: a. 1-tosyl-3-(4'-acetylphenyl)-2-propyne, BF_3-Et_2O; b. excess MCPBA, CH_2Cl_2; c. KF, 18-crown-6, DMF; d. [^{18}F]fluoride, K_2CO_3, 18-crown-6, DMF

Scheme 2.

Table 1

In vitro binding affinities for dithianes and dithiane oxides as in vivo radioligands for the picrotoxin site of the $GABA_A$ receptor. Values shown are the K_i for competition with the radioligand [^{3}H]EBOB binding to rat cortical P3 fractions.

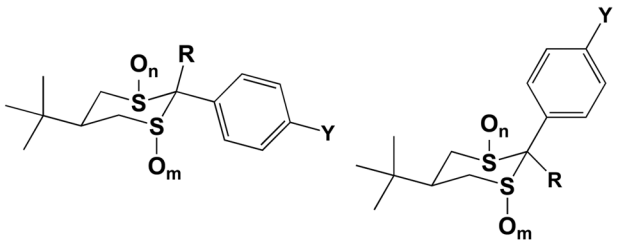

trans-isomer *cis-isomer*

Y	R	m	n	Isomer	K_i (nM)
Br	H	0	0	*trans*	77
Br	H	0	0	*cis*	238
Br	CH_3	0	0	*trans*	181
Br	CH_3	0	0	*cis*	18700
Br	H	2	1	*trans*	90
Br	H	2	2	*trans*	154
Br	CH_3	2	2	*trans*	25
CN	H	0	0	*trans*	9
CN	H	0	0	*cis*	68
CN	CH_3	0	0	*trans*	200
CN	CH_3	2	1	*trans*	139
CN	CH_3	2	2	*trans*	177
$CCCH_2$ F (**1**)	CH_3	2	0	*trans*	6.5 ± 0.3
$CCCH_2$ F (**2**)	CH_3	2	2	*trans*	6.5 ± 0.4

Table 2

Regional brain distributions for compound **1** in CD-1 mouse brain.

Time (min)	% injected dose/g 2	10	30	60
Tissue				
cortex	4.46 ±0.35	3.77 ± 0.18	2.12 ± 0.59	2.28 ± 0.36
cerebellum	4.64 ± 0.63	4.94 ± 0.19	3.02 ± 0.76	3.13 ± 0.47
hippocampus	4.05 ± 0.58	3.39 ± 0.43	2.16 ± 0.52	2.13 ± 0.21
striatum	3.84 ± 0.31	3.39 ± 0.29	1.81 ± 0.32	1.88 ± 0.35
pons	3.74 ± 0.15	2.98 ± 0.74	1.73 ± 0.48	1.54 ± 0.21
thalamus	4.48 ± 0.14	3.66 ± 0.33	1.96 ± 0.49	2.08 ± 0.35
hypothalamus	3.68 ± 0.71	2.82 ± 0.84	1.81 ± 0.41	2.05 ± 0.5
		Tissue/pons		
cortex	1.19 ± 0.06	1.37 ± 0.53	1.23 ± .010	1.48 ± 0.09
cerebellum	1.23 ± 0.15	1.79 ± 0.66	1.77 ± 0.07	2.03 ± 0.08
hippocampus	1.08 ± 0.13	1.18 ± 0.24	1.27 ± 0.14	1.39 ± 0.11
striatum	1.03 ± 0.14	1.22 ± 0.46	1.08 ± 0.14	1.22 ± 0.18
thalamus	1.20 ± 0.08	1.32 ± 0.47	1.15 ± 0.13	1.35 ± 0.09
hypothal	0.98 ± 0.22	1.09 ± 0.72	1.07 ± 0.24	1.32 ± 0.21

Table 3

Regional brain distributions for compound **2** in CD-1 mouse brain.

	% injected dose/g			
Time (min)	**2**	**10**	**30**	**60**
Tissue				
cortex	4.55±0.55	2.25 ± 0.30	1.38 ± 0.24	1.08 ± 0.19
cerebellum	4.23 ± 0.74	2.48 ± 0.37	1.39 ± 0.23	1.01 ± 0.32
hippocampus	3.55 ± 0.41	2 0 ± 0.37	1.18 ± 0.22	0.87 ± 0.16
striatum	3.47 ± 0.86	1.59 ± 0.33	0.94 ± 0.1	0.73 ± 0.21
pons	3.6 ± 0.65	1.82 ± 0.37	0.95 ± 0.13	0.7 ± 0.25
thalamus	4.16 ± 0.60	1.98 ± 0.40	1.14 ± 0.13	0.76 ± 0.05
hypothalamus	2.75 ± 0.21	1.09 ± 0.24	0.750 ± 0.08	0.65 ± 0.26
		Tissue/pons		
cortex	1.36 ± 0.19	1.26 ± 0.11	1.45 ± 0.17	1.65 ± 0.28
cerebellum	1.25 ± 0.19	1.39 ± 0.19	1.47 ± 0.24	1.49 ± 0.11
hippocampus	1.06 ± 0.23	1.11 ± 0.10	1.25 ± 0.28	1.33 ± 0.25
striatum	1.0 ± 0.24	0.88 ± 0.09	0.99 ± 0.08	1.08 ± 0.14
thalamus	1.26 ± 0.25	1.10 ± 0.13	1.21 ± 0.19	1.20 ± 0.33
hypothal	0.84 ± 0.34	0.63 ± 0.23	0.81 ± 0.21	0.93 ± 0.05

Table 4

In vivo regional brain distribution of potential PET radiopharmaceuticals. Every study done in CD-1 mice using standard tissue dissection technique. Time point chosen for maximal differentiation between target and nontarget regions (CTX = cortex, CBL = cerebellum, STR = striatum, HYPO = hypothalamus)

Radioligand (ref)	Target	time (min)	%ID/g (target)	%ID/g (nontarget)	outcome
[^{18}F]dioxodithiane **1**	Pic-GABA$_A$	60	1.08±0.19 (CTX)	0.7±0.25 (PONS)	currrent work
[^{18}F]tetraoxodithiane **2**	Pic-GABA$_A$	60	2.28±0.36 (CTX)	1.54±0.21 (PONS)	currrent work
[^{18}F]FT-BOB [7]	Pic-GABA$_A$	20	1.36±0.38 (CTX)	1.24±0.45 (PONS)	failure
[^{11}C]flumazenil	BzR-GABA$_A$	45	3.34±0.18 (CTX)	0.89±0.31 (CBL)	human studies - good
[^{18}F]PD-1 [28]	GABA transporter	60	0.32±0.03 (CTX)	0.23±0.05 (STR)	failure
[^{18}F]GBR 13119 [29]	DA transporter	60	2.33±0.63 (STR)	0.58±0.13 (CBL)	see GBR 12909
[^{18}F]GBR 12909 [30]	DA transporter	60	2.8±0.11 (STR)	0.66±0.06 (CBL)	human studies- poor
[^{3}H]methylphenidate	DA transporter	30	3.81±0.26 (STR)	1.60±0.10 (CBL)	human studies - good
[^{11}C]nisoxetine [31]	NE transporter	20	1.34±0.75 (HYPO)	0.64±0.61 (STR)	failure
[^{11}C]TRB [32]	mAChR	60	10.5±2.76 (CTX)	1.34±0.17(CBL)	human studies - good
[^{11}C]NMPB [33]	mAChR	60	10.4±0.52 (CTX)	1.13±0.10(CBL)	human studies-better
[^{11}C]NMPYB [34]	mAChR	60	8.72±0.46 (CTX)	1.49±0.12(CBL)	best-human in future?
3-[^{18}F]FEPB [35]	mAChR	60	3.17±0.22 (CTX)	2.52±0.25(CBL)	failure
4-[^{18}F]FEPB [35]	mAChR	60	2.81±0..40 (CTX)	1.37±0.17(CBL)	good
[^{11}C]metanicotine [36]	nAChR	40	2.48±0.48 (THAL)	2.43±0.42 (CBL)	failure
[^{11}C]E2020 [37]	AChE	30	1.84±0.24 (STR)	1.64±0.32 (HYPO)	failure
[^{11}C]benzisoxazole [38]	AChE	40	3.58±1.03 (STR)	4.98±1.5 (PONS)	failure
[^{11}C]MABV [39]	VAChT	45	3.99±0.22 (CTX)	1.05±0.25 (CBL)	good
[^{18}F]FEOBV [40]	VAChT	240	3.30±0.56 (CTX)	1.19±0.37 (CBL)	IND in progress
[^{11}C]TBZ [41]	VMAT2	10	4.96±1.0 (STR)	1.76±0.36 (CBL)	human studies - good
[^{11}C]MTBZ [42]	VMAT2	15	4.19±0.5 (STR)	1.42±0.07 (CBL)	human studies-better
(+)-[^{11}C]DTBZ [43]	VMAT2	15	8.31±0.61 (STR)	2.73±0.10 (CBL)	human studies - best
[^{11}C]Carfentanil [44]	mu opioid	15	3.05±0.22 (STR)	0.93±0.25 (CBL)	human studies good
[^{11}C]2-Me-carfentanil [44]	mu opioid	15	3.59±0.55 (STR)	0.88±0.09 (CBL)	better than CFN?
[^{11}C]SNC 80 [45]	delta opioid	40	0.88±0.15 (CTX)	0.72±0.15 (PONS)	failure